Fusion cross sections in systems leading to ^{170}Hf at near-barrier energies

S. Gil, F. Hasenbalg, J. E. Testoni,* D. Abriola, M.C. Berisso, M. di Tada, A. Etchegoyen,* J.O. Fernández Niello,* and A.J. Pacheco*

Laboratorio TANDAR, Departamento de Física, Comisión Nacional de Energía Atómica, Avenida del Libertador 8250, 1429 Buenos Aires, Argentina

A. Charlop, A.A. Sonzogni, and R. Vandenbosch

Nuclear Physics Laboratory, University of Washington, Seattle, Washington 98195

(Received 2 May 1994; revised manuscript received 15 November 1994)

In an effort to study the effect of the entrance channel mass asymmetry on the fusion process at near-barrier energies, we have measured the fusion cross section and its distribution according to the different evaporation residues for the ^{28}Si $+^{142}$Ce, ^{32}S $+^{138}$Ba, and ^{48}Ti $+^{122}$Sn systems. All these systems lead to the same compound nucleus ^{170}Hf. The measurements were performed using a delayed x ray technique. For the last two systems we have also measured the fission cross sections in the same bombarding energy range. This experimental information can be used to restrict the free parameters of the statistical model used to account for the relative yield. A constrained and realistic statistical decay model is useful in reducing the uncertainties in the determination of the spin distribution from measurements of gamma multiplicities for these systems. The excitation function for the fusion cross section can be described using a schematic coupled channels calculation with realistic coupling strengths. Our results show no unambiguous effect that can be associated with the entrance channel mass asymmetry .

PACS number(s): 25.70.Jj, 24.10.Eq

I. INTRODUCTION

The discovery of large enhancements of the fusion cross section near and below the Coulomb barrier in a great number of reactions between heavy ions (HI), relative to expectations from a one-dimensional barrier-penetration model, has induced a renewed interest in the study of near and sub-barrier fusions [1,2]. Considerable progress has been achieved in understanding the enhancement of the fusion cross section by including new degrees of freedom such as static and dynamic deformation and nucleon transfer. These effects reveal an interesting and rich interplay between the dynamics of the reaction and the structure of the participant nuclei [2,3]. Despite the success of these approaches in explaining the enhancement of the fusion cross section in many systems, some questions about the spin distribution of the compound nucleus (CN) formed in these reactions still remain open. For some systems, these models seem to succeed in reproducing both the fusion excitation functions and the shape of the spin distributions. In other cases, particularly for heavier and more symmetric systems, the experimental spin distributions are broader than those predicted by the same models even though the cross sections are still well described. Definite conclusions in this respect are further complicated by possible systematic uncertainties arising from the fact that different techniques for the extraction of the spin distribution have been applied for different systems. A comprehensive review of these points may be found in Ref. [4].

A common assumption in most of the proposed models for describing the fusion process is that the inertial parameter used in the calculation is given by the reduced mass of the system. It is well known that the reduction of a two-body to a one-body problem, with mass equal to the reduced mass of the system, is valid whenever the separation of the two bodies is larger than their own dimensions. In heavy and symmetric systems there is a considerable overlap of participant nuclei at the distance where the interaction potential is maximum. Given the relevance of the inertia parameter in affecting the spin distribution of the CN [5,6] it seems interesting to do a systematic measurement of both the fusion cross section and the spin distribution of the CN for different combinations of projectiles and targets that lead to the same CN. Incidentally, there have been theoretical predictions of important deviations of the inertial parameter with respect to the classical reduced mass when the colliding nuclei overlap. Using an adiabatic time-dependent Hartree Fock approach [7,8] in very light systems it was shown that in these cases, the inertial parameter associated with the relative motion of the interacting nuclei increases by a large factor with respect to the reduced mass. This effect may be interpreted as a consequence of the Pauli principle. As the two Fermi systems overlap, the more peripheral nucleons need to occupy higher excited states, this gain of internal excitation energy is achieved at the expense of the loss of energy in the relative motion which can be simulated by an increase in

*Member of the Consejo Nacional de Investigaciones Científicas y Tecnicas (CONICET), Argentina.

the inertia parameter. Therefore, by varying the mass asymmetry of the entrance channel, the nuclear interaction and the overlap change, thus making observable this exotic effect on the inertial parameter. Furthermore, the simultaneous study of such different systems, with varying mass asymmetry in the entrance channel, also reduces the uncertainties in extracting the spin distribution information from measurements of γ-ray multiplicities [9,10]. Another interesting question that could be addressed in these studies is the role of the size of the Coulomb barrier (proportional to $Z_{\text{projectile}} \cdot Z_{\text{target}}$) in the fusion process at near-barrier energies. It is expected that in these complex systems several degrees of freedom will be involved in the fusion process.

A comprehensive set of experimental information on the fusion process of systems with various mass asymmetries in the entrance channel would result in an adequate testing ground for theoretical models that include quantum mechanical tunneling in several dimensions. These measurements would also be useful in testing an alternative description of sub-barrier fusion enhancements where the neck formation degree of freedom is emphasized. According to recent theoretical calculations these effects would be more pronounced in the heavier and symmetric systems [11].

The systems we have studied are ^{28}Si $+^{142}$Ce, ^{32}S $+$ ^{138}Ba, and ^{48}Ti $+^{122}$Sn. They all lead to the same compound nucleus ^{170}Hf, while the reduced masses of the entrance channel as well as the Coulomb barriers vary by about 50% between the most asymmetric and the most symmetric systems. Neutron evaporation is the main decay mode of the compound nucleus produced at near-barrier energies for these reactions. The evaporation residues produced in these reactions are radioactive, with lifetimes of a few minutes. Since the primary decay mode is electron capture for these evaporation residues it is possible to use a delayed x-ray technique to determine not only the fusion cross sections for these systems, but also the fractionation into the different decay channels (xn, xn-α, etc.) at each energy. This fractionation of the fusion cross section depends on properties associated with (a) the characteristics of the compound system and its decay channels such as level densities, intensity of electromagnetic transitions, fission barriers, etc. (these parameters are the same for all our systems) and (b) properties determined by the entrance channel: excitation energy and spin distribution. These latter quantities depend, among other things, on the coupling strengths of the colliding nuclei, the interaction barrier, and the reduced mass of the entrance channel. Therefore it is expected that these experimental data will help to disentangle these aspects of the fusion process.

Finally, the fact that the residual nuclei produced in all these reactions have the characteristics of good rotors makes the use of conventional γ-ray multiplicity techniques particularly useful for extracting information about the spin distribution of the CN. The results of γ-ray multiplicity measurements for these systems will be reported in a separate paper [12]. A summary of some of these results has been reported in a recent Rapid Communication [13].

II. THE EXPERIMENT

The experimental techniques used in this work have been previously described in Ref. [14]. Beams of ^{28}Si, ^{32}S, and ^{48}Ti were produced by the 20-UD tandem accelerator of the TANDAR Laboratory in Buenos Aires. The targets used in each of the three reactions were ^{142}Ce (83.10%), ^{138}Ba (99.67%), and ^{122}Sn (92.20%) with thicknesses of 48±3 μg/cm^2, 85±2 μg/cm^2, and 169±4 μg/cm^2, respectively, all produced by evaporation onto thin carbon foils of about 20 μg/cm^2. The uncertainty in the beam energy was less than 1% [15]. An aluminum catcher foil was placed at about 2 mm down stream from the target. The thicknesses of these catchers were 1.6 mg/cm^2, 2.5 mg/cm^2, and 3.2 mg/cm^2 for the targets of ^{142}Ce, ^{138}Ba, and ^{122}Sn, respectively. These thicknesses were chosen so that the evaporation residues produced in the reactions of interest would be stopped in the catcher, but not those produced in the reactions with the carbon backing and the aluminum from the catcher itself. Two surface barrier detectors, placed at ±30° with respect to the beam direction, were used as monitors for normalization purposes. The beam was collected in a Faraday cup. The profile of the beam current was monitored and recorded in time intervals of 1 min. For the three systems studied, the beam currents varied between 50 and 200 nA.

At the highest bombarding energy for each reaction, a second catcher was used in order to corroborate that no residual product from the main reaction was escaping from the first catcher.

The irradiations were carried out for about 1 – 2 hr. For some selected bombarding energies, shorter irradiations of about 30 min were also carried out to enhance the sensitivity of the technique to the short lifetime residual nuclei. After the irradiation, the catchers were removed from the scattering chamber and placed in front of a 13.2 cm^3 high purity germanium (HPGe) detector. This operation was achieved in 4 min or less. The energy resolution of the HPGe was 0.58 keV (FWHM) at 50 keV. Two positions were used to place the catchers in front of the detector; a close configuration (position No. 1) at about 2.75 mm from the detector window and a far configuration (position No. 2) at 5.98 cm from the window of the HPGe. The far configuration was used at the beginning of the measurements when the catcher was too active to be placed in the closer position. After the activity of the catcher had decayed, we moved it to the close position to improve the counting statistics. The absolute efficiency of the detector was measured at both positions using calibrated γ sources. At 50 keV the absolute photopeak efficiencies were 18% in the close position and 1.5% in the far one. Since the useful energy range of the detector spanned from E_γ=20 – 240 keV, several γ-rays from the decay of the evaporation residues could also be detected in addition to the x rays. The γ-decay information was used to complement and test the conclu- of the x rays. The decay activity of the catchers were followed for the first 2 hr immediately after the irradiation, and whenever possible, for about 2 hr more one day after the irradiation. The counting sequence consisted, typi-

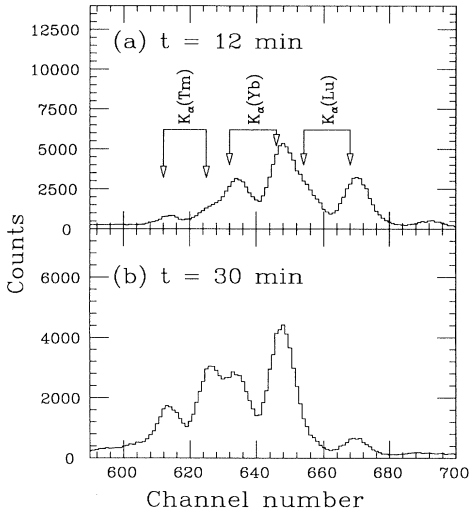

FIG. 1. A portion of the spectrum from the radioactive decay of the evaporation residues, from the reaction $^{32}S + ^{138}Ba$ at E_{lab}=165 MeV (a) 12 min and (b) 30 min after the end of the irradiation.

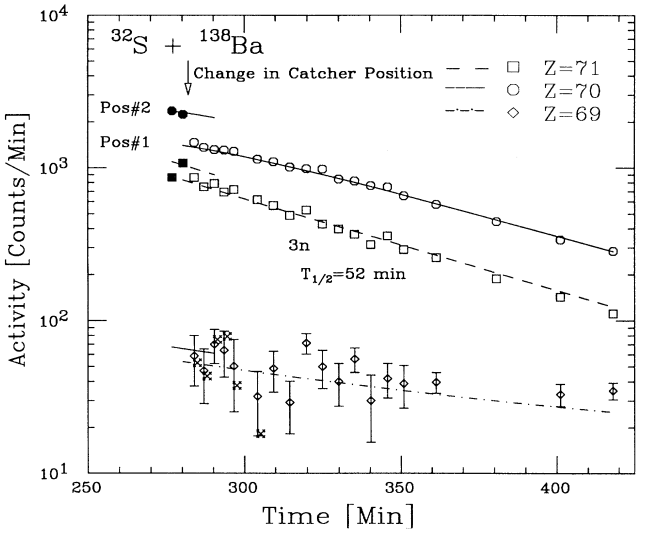

FIG. 2. Off-line time dependence of the activity from the radioactive decay of the evaporation residues, from the reaction $^{32}S + ^{138}Ba$ at E_{lab}=125 MeV. The lines correspond to the XRAY-code calculations.

cally, of 5 measurements of 3 min duration, followed by 5 measurements of 5 min, and another 5 measurements of 15 min. The area of the K_{α_1} and K_{α_2} peaks for the different Z values involved were obtained using the fitting code GASPAN [16]. For each Z the K_{α_1} and K_{α_2} peaks were accepted only if they had the correct energy and their relative intensities were in agreement with the expected ratios ($K_{\alpha_2}/K_{\alpha_1} \approx 0.57$), in such cases they were added. Figure 1 shows typical x-rays spectra at two different times, for a given run. Corrections for electronic dead time were determined using a pulse generator. The evaporation residues cross section (σ_{ev}) was obtained by summing the yields of the individual light-particle evaporation channels (σ_A). These individual cross sections were obtained through a χ^2 minimization procedure using the computer code XRAY [17]. The procedure consists of comparing the observed time dependence of the K_α intensities with the *a priori* expectations, assuming that the lifetimes ($T_{1/2}$) and the number K_α x rays produced every 100 decay of the parent nucleus ($W_{Z,A}$) involved are known.

An additional correction for summing effects was necessary, particularly for the spectra obtained in the closer position (No. 1). In this case, due to the large total efficiency of the detector, it is possible that more than one photon arrives at the detector in coincidence. Therefore, one would expect that for the close position, once the data have been corrected by efficiency differences and dead times, the areas of the peaks in position No. 1 would lay below than those corresponding to position No. 2. This is evident in the data as seen in Figs. 2 and 3, where the experimental data points are corrected only by detector efficiency. The summing correction factors were obtained by the following procedure: first, an *a priori* estimation of the summing correction factor was done for those nuclei for which the decay schemes are well known. Second, a fine tuning of these values was achieved by requiring that the theoretical predictions of the time dependence of the x-ray intensities reproduce the discontinuity at the change of position of the catcher. Since the changes of position occurred at different times for each bombarding energy, in most of the cases the discontinuity for each Z is usually dominated by a few A values (often just one A). Therefore, by requiring a reproduction of the discontinuities for all the bombarding energies, the relevant set of summing correction factors can be evaluated within a few percent. A good agreement with the *a priori* estimation is obtained whenever the decay scheme

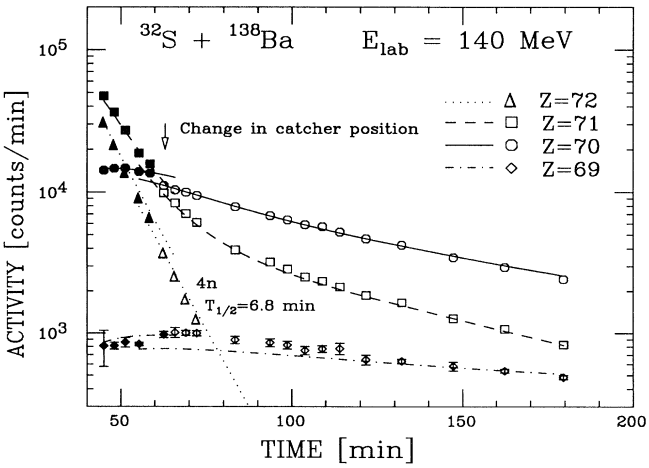

FIG. 3. Off-line time dependence of the activity from the radioactive decay of the evaporation residues, from the reaction $^{32}S + ^{138}Ba$ at E_{lab}=140 MeV. The lines correspond to the XRAY-code calculations.

TABLE I. Input information used for extracting the fusion cross sections. $T_{1/2}$ is the half life in minutes, $W_{Z,A}$ the number of K_α x rays produced per 100 decays of the parent, and SCF is the summing correction factor used in the close position (No. 1).

	Z					
	72	71	70	69	68	A
$T_{1/2}$	25.9	6.7				168
$W_{Z,A}$	100	80				
SCF	0.85	0.8				
$T_{1/2}$	2.05	51.5	17.5	13,320.		167
$W_{Z,A}$	39.0	79.5	149.	75.9		
SCF	0.85	0.80	0.60	0.95		
$T_{1/2}$	6.77	2.37	3,398.	462.		166
$W_{Z,A}$	74.2	56	109.7	85.4		
SCF	0.68	0.63	0.9	0.8		
$T_{1/2}$	1.7	10.87	9.9	1803.	621.6	165
$W_{Z,A}$	64	79	82.8	81.2	60.3	
SCF	0.9	0.78	0.95	0.8	1.0	
$T_{1/2}$	2.8	3.14	75.6	2.0		164
$W_{Z,A}$	64	77	65.	46.2		
SCF	0.9	0.8	0.8	0.8		
$T_{1/2}$			11.1	108.6	75.	163
$W_{Z,A}$			57.7	115.7	62.6	
SCF			0.93	0.6	1.0	
$T_{1/2}$			18.9	22.73		162
$W_{Z,A}$			66.8	73.8		
SCF			0.9	0.95		

is well known. This procedure was carried out for all the energies employed in the system $^{32}S + ^{138}Ba$ and for a few selected energies in the other systems. In all cases the discontinuity at the change of position is very well reproduced as can be seen in Figs. 2 and 3.

In the few cases for which the $W_{Z,A}$ were not known, they were estimated by the following procedure. If a $W_{Z,A}$ was not known for a given exit channel characterized by A, and if a γ ray in this same decay chain can be found with known absolute intensity, then σ_A was estimated using both the time dependence and the intensity of this particular γ ray. Once σ_A was found, the value

TABLE II. Fusion cross sections for $^{28}Si + ^{142}Ce$ and their fractionation into the different decay modes. σ_{fiss} are results from PACE calculations as described in the text.

E_{lab} (MeV)	σ_{fus} (mb)	σ_{2n}	σ_{3n}	σ_{4n}	σ_{5n}	σ_{6n}	$\sigma_{xn\alpha}$	σ_{fiss} (mb)
104.7	0.07 ± 0.03		0.07					
106.7	0.33 ± 0.15		0.30	0.03				
107.2	0.6 ± 0.1	0.07	0.47	0.02				
108.2	1.2 ± 0.1		0.97	0.26				
108.7	2.0 ± 0.2	0.12	1.20	0.29			0.42	
109.7	3.7 ± 0.3	0.07	2.32	1.06			0.22	
112.2	14.4 ± 0.8	0.54	5.86	3.60	2.78		1.60	
112.2	14.2 ± 0.5	0.51	6.45	3.28	2.50		1.45	
114.7	34 ± 3		12.1	13.4	4.33		4.55	
114.7	39 ± 2	1.02	13.0	13.7	7.67		3.19	
117.2	71 ± 1		17.7	36.7			16.5	
119.7	146 ± 6		23.7	71.7	18.4		32.6	
119.7	134 ± 7		21.9	75.0	26.1		11.5	
124.7	244 ± 7		21.0	146	44.6	22	9.82	
124.7	235 ± 5		19.1	138	38.3	11	28.3	
124.7	242 ± 5		21.6	143	42.0	11	24.3	
129.7	429 ± 12		15.0	218	91	66	37.5	
129.7	449 ± 6		19.5	239	100	51	39	
139.7	719 ± 90		7.7	190	328	48	125	20[a]
144.7	644 ± 30		5.0	102	238	86	165	48[a]

[a]Fission cross section estimated from statistical model calculations.

TABLE III. Fusion cross sections for $^{32}S + ^{138}Ba$ and their fractionation into the different decay modes. σ_{fiss} were measured by Charlop *et al.* [12].

E_{lab} (MeV)	σ_{fus} (mb)	σ_{2n}	σ_{3n}	σ_{4n}	σ_{5n}	σ_{6n}	$\sigma_{xn\alpha}$	σ_{fiss} (mb)
122.2	0.5 ± 0.2	0.04	0.32	0.05			0.04	
123.2	1.4 ± 0.2	0.15	0.97	0.12			0.16	
124.7	3.2 ± 0.5	0.3	2.2	0.35			0.4	
127.2	11.9 ± 0.4	0.01	4.8	5.9	0.3		0.9	
129.7	22 ±0.5		8.8	11	0.8		1.3	
132.2	47±1.7		12.4	29	1		3.5	
134.7	80 ±5		15.3	51	7.3		5.7	
139.7	191 ± 6		16	146	19	5.4	4.1	1[a]
144.7	262 ±10		12.3	172	60	6	10	2[a]
149.7	398± 12		9.5	193	159	1.4	30	5
154.7	490 ± 30			170	233	37	35	15
159.7	538 ± 20			116	231	63	90	38
164.7	551± 25			68	258	77	75.5	72

[a]Fission cross section extrapolated from measured values.

of the unknown $W_{Z,A}$ was estimated by requiring that the theoretical prediction of the time dependence of the x-ray intensities be well reproduced for the value of σ_A obtained from γ rays. This procedure needs to be done only once and for the more favorable bombarding energy and system. In Table I we show the values of W's and summing correction factors (for position No. 1) for the nuclei of relevance in this study.

III. RESULTS AND DISCUSSION

The results of the fractionation of the fusion cross section into the different channels are summarized in Tables II – IV, together with the total evaporation residues. In these tables we also show the results of the measured fission cross sections for the systems $^{32}S + ^{138}Ba$ and $^{48}Ti + ^{122}Sn$ [18]. The values of the fission cross sec-

TABLE IV. Fusion cross sections for $^{48}Ti + ^{122}Sn$ and their fractionation into the different decay modes. σ_{fiss} were measured by Charlop *et al.* [12].

E_{lab} (MeV)	σ_{fus} (mb)	σ_{2n}	σ_{3n}	σ_{4n}	σ_{5n}	σ_{6n}	$\sigma_{xn\alpha}$	σ_{fiss} (mb)
169.1	2.3 ±0.2	0.6	1.2	0.13			0.42	
170.1	4.7 ±0.3	0.8	2.4	0.8			0.7	
171.1	13.4 ±0.6	1.7	6.6	2.1			3.1	
174.1	17.8 ±1.5	1.8	9	3.2	1		1.6	
174.1	18 ± 1	1.9	9.8	3.1	1.25		1.8	
174.1	18.3 ±1	2.05	9.9	3.4	1.13		1.8	
176.1	30 ±1.3	2.3	15	8	1.9		3	
179.1	56±2	3.6	23	20	3.9		5.9	
179.1	57 ±5	3.8	23.3	20.5	3.8		5.6	
184.1	133 ±5	6	38	67.5	8.7		12.8	
189.1	172 ± 9	6.3	30.5	99	14		21	2[a]
189.1	179 ± 4	6.3	37.	99	14		21	2[a]
194.1	278 ± 10	4.6	41.5	154	33.5	20	15	9[a]
199.1	294 ± 15		27	137	47	10	37	36
204.1	465 ± 25		20	193	107	20	45	80 [a]
209.1	485 ± 35		7.4	130	141	20	53.5	133
214.1	587 ± 55		1.6	96	175	40	69	205[a]
219.1	635 ±60			50	191	51	82	261
222.1	850 ± 150			91	246	70	146	300[a]

[a]Fission cross section extrapolated from measured values.

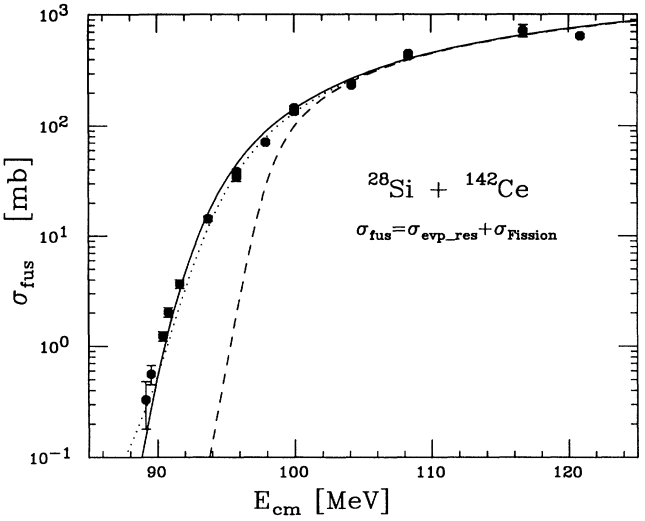

FIG. 4. Fusion cross section versus center-of-mass energy for the system ^{28}Si+^{142}Ce. The solid line is a CCDEF fit with the parameters indicated in the text. The dotted line is the result obtained using the alternative parameters indicated in Table V. The dashed curves are the result of CCDEF with all couplings removed.

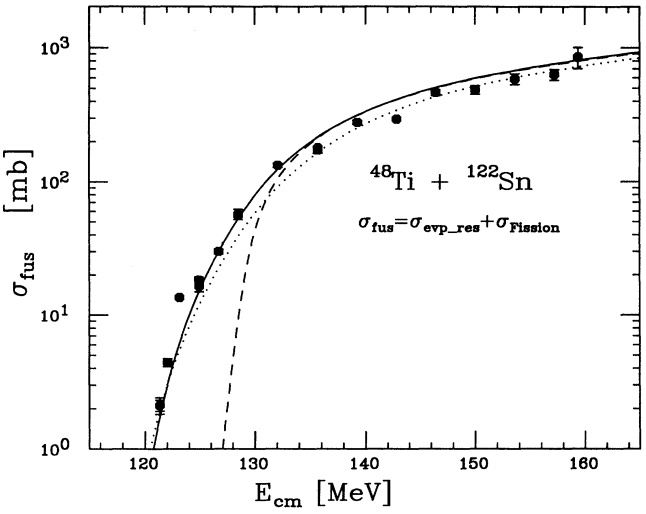

FIG. 6. Fusion cross section versus center-of-mass energy for the system ^{48}Ti+^{122}Sn. The solid line a CCDEF fit with the parameters indicated in the text. The dotted line is the result obtained using the alternative parameters indicated in Table V. The dashed curves are the result of CCDEF with all couplings removed.

tion for the system ^{28}Si +^{142}Ce were not measured, but the expectation of a reliable statistical model calculation, as discussed below, indicates that fission is negligible for this system for all energies studied here, except for the two higher ones. The quoted values of the fission cross section for these two energies are obtained from the statistical model code PACE [19].

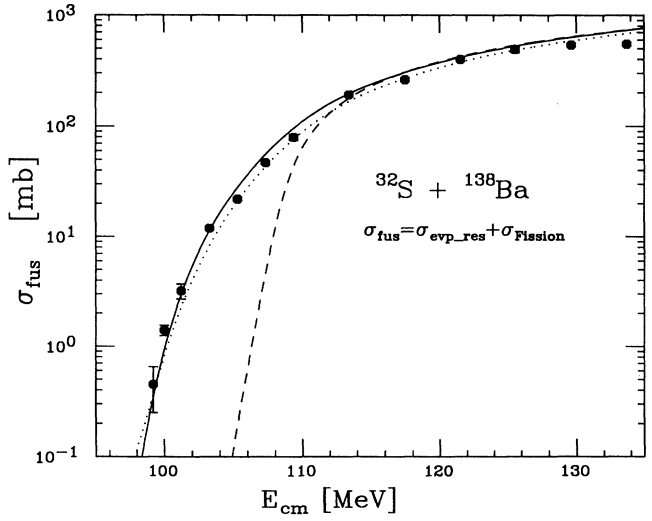

FIG. 5. Fusion cross section versus center-of-mass energy for the system ^{32}S+^{138}Ba. The solid line is a CCDEF fit with the parameters indicated in the text. The dotted line is the result obtained using the alternative parameters indicated in Table V. The dashed curves are the result of CCDEF with all couplings removed.

Excitation functions of the fusion cross section versus those of the center-of-mass energy are displayed in Figs. 4, 5, and 6 for the systems ^{28}Si +^{142} Ce, ^{32}S +^{138} Ba, and ^{48}Ti +^{122} Sn, respectively. The solid curves in these figures are the results of calculations using a schematic and simplified coupled channels model, CCDEF [20]. This model allows for the coupling of static deformation, surface vibrational states, and nucleon transfer. In the present calculation we have included the coupling to the first 2^+ and 3^- states for both target and projectile. The parameters used in these calculations are summarized in Table V. In the three systems studied, the projectiles were considered as having a permanent quadrupole deformation. The couplings to the first 3^- states of both projectile and target and to the first 2^+ of the target were included as vibrational excitations. The values of the coupling parameters were obtained from the literature [21,22]. We have also included in this calculation the effect of a nucleon transfer channel. Since little is known about transfer in these systems, we have made the following estimates. In a first approach we considered one-nucleon transfer only. The Q value in this case corresponds to that of one-neutron pickup to the ground state. This channel was chosen as the most favorable based on Q values for single nucleon transfer. The form factor used for the coupling was that corresponding to the default single nucleon transfer form factor of 1.0. The only adjustable parameter used in these CCDEF calculations was the depth of the nuclear potential. This parameter was adjusted so as to obtain a good overall fit of the data. The results of these calculations are shown as the solid curves in Figs. 4, 5, and 6. We have also performed an alternative calculation, using the same vibrational and rotational states and couplings

TABLE V. Parameters used in CCDEF calculations. The first seven rows indicate the input parameters. The double columns under each system indicate the strength values associated with the projectile (left) and target (right).

	^{28}Si +^{142}Ce		^{32}S +^{138}Ba		^{48}Ti +^{122}Sn	
	Input parameters					
β_2	- 0.41	0.12	0.31	0.09	0.27	0.10
E_x(MeV)	1.78	0.64	2.23	1.44	0.983	1.14
β_3	0.40	0.13	0.48	0.13	0.19	0.12
E_x(MeV)	6.88	1.65	5.01	2.88	3.36	2.49
Transfer FF(1n)	1.0		1.0		1.0	
Q_{transf}(MeV)	+1.31		+0.03		-0.67	
DV (MeV)	1.0		0.0		6.8	
	Output parameters					
V_b (MeV)	98.7		108.2		128.8	
R_b (fm)	11.05		11.11		11.51	
r_b (fm)	1.34		1.33		1.34	
$\hbar\omega$ (MeV)	4.00		3.88		3.68	
	Input parameters - Alternative fit					
Transfer FF(1n)	1.3		1.8		3.5	
Q_{transf}(MeV)	+1.31		+0.03		-0.67	
Transfer FF(2n)	0.5		0.6		0.8	
Q_{transf}(MeV)	+6.49		+4.55		4.09	
DV (MeV)	10		-6.0		-4.0	
	Output parameters					
V_b (MeV)	97.5		109.3		130.7	
R_b (fm)	11.23		10.95		10.81	

as before, but including the 2-neutron pick-up channels which have large and positive Q values in these systems. The form factors for 2-nucleon transfer are usually considerably smaller than those for 1-nucleon transfer. The inclusion of these channels with a strength based on the prescription of [23] increases the fusion cross section at the lower energies and results in a kink in the excitation function which is not observed in the data. The absence of a kink in the data bounds the magnitude of these form factors.

We have reduced the amplitude of the 2n transfer by about a factor of 3 to obtain an acceptable fit to the excitation function. The need for this reduction is not surprising as it has been shown in [24] that the approximations involved in CCDEF lead to an overprediction of the fusion cross section for very positive Q values. The dotted curves in Figs. 4, 5, and 6 were obtained using the alternative parameters indicated in Table V. In these alternative calculations the form factors for 1n and 2n transfer were treated as adjustable parameters in addition to the depth of the nuclear potential. The improvement of the fit in the knee region is primarily due to the increased strength of the 1n transfer form factor. It is also interesting to note that the average angular momentum obtained by these two different parametrizations differ by less than 15%.

The results for the relative channel yields, i.e., the fractionation of the fusion cross section, Y_n, into the different fusion evaporation residues, are presented in Figs. 7, 8, and 9, as a function of the excitation energy of the compound nucleus ^{170}Hf. In these figures the continuous lines show the prediction of the relative yields by the statistical evaporation code PACE [19]. Some of the input parameters of this model depend on properties of the

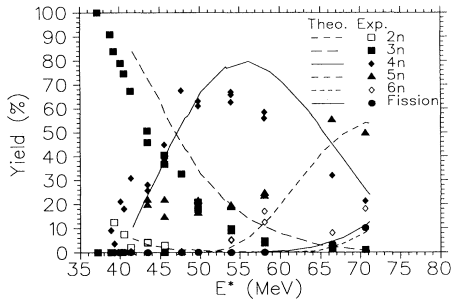

FIG. 7. Percentage of the relative yield as a function of the excitation energy of the compound nucleus ^{170}Hf, for the system ^{28}Si +^{142}Ce. The continuous curves result from a statistical model calculation (PACE), with the parameters indicated in the text.

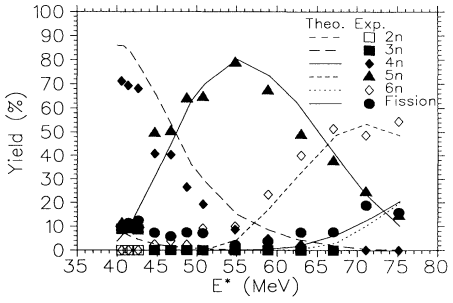

FIG. 8. Percentage of the relative yield as a function of the excitation energy of the compound nucleus ^{170}Hf, for the system ^{32}S+^{138}Ba. The continuous curves result from a statistical model calculation (PACE) with the parameters indicated in the text.

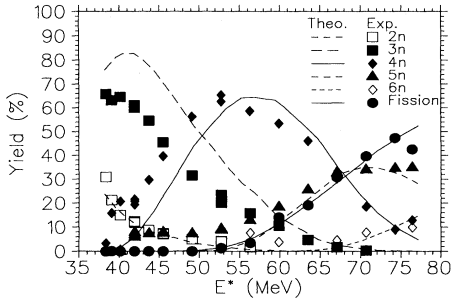

FIG. 9. Percentage of the relative yield as a function of the excitation energy of the compound nucleus ^{170}Hf, for the system ^{48}Ti + ^{122}Sn. The continuous curves result from a statistical model calculation (PACE) with the parameters indicated in the text.

compound system produced in these reactions. Therefore, these parameters were held constant for the three systems. The level density parameters used in the calculation were $a_n = A/9$ (MeV^{-1}) and a_n/a_f=1. The reduced γ-transition strengths were 0.01, 9.0, and 1.2 W.u. for the statistical $M1$, $E2$, and $M2$ transitions, respectively. For the statistical $E1$ strength the default value of 1.4 was the fraction of the sum rule exhausted by the integrated $E1$ strength, whereas for the strength of the collective $E2$ transitions we have used 10.0 W.u. Discrete levels up to 2.0 MeV were introduced for all the nuclei involved in the decay, whenever this information was available. The spin distributions used in all cases were those obtained from a CCDEF calculation, which gave a good fit to the excitation function for each system as described above. There is an overall agreement between the statistical model predictions and the experimental results for the relative yields; however, the large α-xn yields obtained in this experiment were systematically underestimated by the model. Reasonable variation of the input parameters never produced yields for the α-xn channel that exceeded 10%. In particular the Y_{xn} for the system ^{32}S + ^{138}Ba is very well described by the statistical model, whereas for the other two systems the fit is less satisfactory. All attempts to vary the input parameters over a realistic range did not improve the fit to the data significantly.

The success of the schematic coupled channel model CCDEF to reproduce the fusion data including only the known structural parameters of the nuclei involved in these reactions suggests that the underlying assumption of using the reduced mass as the inertia parameter in the fusion processes studied here is reasonable. Therefore, our results do not show a clear indication of the existence of any unexpected entrance channel effect beyond those included in CCDEF. Similarly, we find no evidence for an effect that can be unambiguously attributed to other processes such as neck formation [11].

IV. CONCLUSIONS

Fusion cross sections have been measured for the three systems ^{28}Si+^{142}Ce, ^{32}S+^{138}Ba, and ^{48}Ti+^{122}Sn, leading to the same compound nucleus, ^{170}Hf. The bombarding energies spanned a range from 20% above to 10% below the Coulomb barrier for each system. Statistical models give a fair description of the fractionation of the fusion products into the different decay modes, even though there is a consistent underprediction of the α-xn channels. Schematic coupled channel calculations using the code CCDEF, including the known coupling strengths for the participant nuclei reproduce reasonably well the fusion cross-section data. Our results show no need to invoke any exotic effect that may be associated with the mass asymmetry degree of freedom. Also these results suggest that it is adequate to use the reduced mass as the inertial parameter for describing the fusion process in these systems.

This work was supported in part by the United States-Argentina Cooperative Program sponsored by the CONICET (Argentina) and the National Science Foundation (U.S.).

[1] M. Beckerman, Phys. Rep. **129**, 145 (1985).
[2] S. Landowne, *Proceedings of the Symposium on Heavy Ion Interactions Around the Coulomb Barrier*, Legnaro, Italy, 1988 (Springer-Verlag, Berlin, 1988), p.3.
[3] S.G. Steadman and M. Rhoades-Brown, Annu. Rev. Nucl. Sci. **36**, 649 (1986).
[4] R. Vandenbosch, Annu. Rev. Nucl. Sci. **42**, 447 (1992).
[5] S. Gil, in *Nuclear Structure and Heavy-Ion Reaction Dynamics 1990*, Institute of Physics Conference Series Number 109, edited by R.R. Betts and J.J. Kolata (Bristol, Philadelphia, 1991), pp. 33–51.
[6] S. Gil, R. Vandenbosch, A.J. Lazzarini, D.-K. Lock, and A. Ray, Phys. Rev. C **31**, 1752 (1985).
[7] H. Flocard, P.H. Heenan, and D. Vautherin, Nucl. Phys. **A339**, 336 (1980).
[8] P.H. Heenan, H. Flocard, and D. Vautherin, Nucl. Phys. **A394**, 525 (1983).
[9] S. Gil, R. Vandenbosch, A. Charlop, A. Garcia, D.D. Leach, S.J. Luke, and S. Kailas, Phys. Rev. C **43**, 701 (1991).
[10] S. Gil *et al.*, Phys. Rev. Lett. **65**, 3100 (1990).
[11] C.E. Aguiar, A.N. Aleixo, W.C. Barbosa, L.R. Canto, and R. Donangelo, Nucl. Phys. **A472**, 571 (1987).
[12] A. Charlop, J. Bierman, Z. Drebi, A. Garcia, S. Gil, D. Prindle, A. Sonzogni, R. Vandenbosch, and D. Ye, Phys. Rev. C **51**, 628 (1995).
[13] A. Charlop *et al.*, Phys. Rev. C **49**, R1235 (1994).
[14] D.E. DiGregorio *et al.*, Phys. Rev. C **39**, 516 (1989).
[15] A.M.J. Ferrero *et al.*, Nucl. Instrum. Methods Phys. Res. Sect. B **42**, 389 (1989).
[16] F. Riess (private communication).
[17] A.J. Pacheco, D.E. DiGregorio, J.O. Fernandez-Niello,

and M. Elgue, Comput. Phys. Commun. **52**, 93 (1988).
[18] A. Charlop, J. Bierman, Z. Drebi, S. Gil, A. Sonzogni, R. Vandenbosch, and D. Ye, Phys. Rev. C **51**, 623 (1995).
[19] A. Gavron, Phys. Rev. C **21**, 230 (1980).
[20] J.O. Fernandez-Niello, C. Dasso, and S. Landowne, Comput. Phys. Commun. **54**, 409 (1989).
[21] S. Raman, C.H. Malarkey, W.T. Milner, C.W. Nestor, Jr., and P.H. Stelson, Nucl. Data Tables **36**, 1 (1987).
[22] R. Spear, Nucl. Data Tables **42**, 55 (1989).
[23] R. Broglia, C. Dasso, and S. Landowne. Phys. Rev. C **32**, 1426 (1985).
[24] C.H. Dasso and S. Landowne, Phys. Lett. B **183**, 141 (1987).